N90-12473

Observational Goals for Max '91 to Identify

the Causative Agent for Impulsive Bursts

D. A. Batchelor (NASA/GSFC)

Recent studies of impulsive hard X-ray and microwave bursts suggest that a propagating causative agent with a characteristic velocity of order 1000 km s^{-1} is responsible for these bursts. In this presentation, the results of those studies will be summarized and observable distinguishing characteristics of the various possible agents will be highlighted, with emphasis on key observational goals for Max '91 campaigns. The most likely causative agents suggested by the evidence are shocks, thermal conduction fronts, and propagating modes of magnetic reconnection in flare plasmas (although other possible agents cannot as yet be ruled out). With the new instrumentation planned for Max '91, high spatial-resolution observations of hard X-ray sources have the potential to identify the agent by revealing detailed features of source spatial evolution. Coordinated observations with the Very Large Array and other radio imaging instruments are also obviously of great importance, as well as detailed modeling of coronal loop structures to place limits on density and temperature profiles in the loops. With the combined hard X-ray and microwave imaging observations, aided by loop model results, the simplest causative agent to rule out would be the propagating modes of magnetic reconnection. To fit the observational evidence, reconnection modes would need to travel at approximately the same velocity (the Alfvén velocity) in different coronal structures that vary in length by a factor of 10^3. Over such a vast range in loop lengths, it is difficult to believe that the Alfvén velocity is constant. Thermal conduction fronts would be suggested by sources that expand along the direction of **B** and exhibit relatively little particle precipitation. Particle acceleration due to shocks could produce more diverse radially expanding source geometries with precipitation at loop footpoints.

I. INTRODUCTION

The main objective of research on solar and stellar flares is the discovery of the process responsible for the unpredictable, rapid, enormous releases of energy that occur in flares. The clearest observational clues are the impulsive X-ray and microwave radiations emitted during flares because these radiations offer the most direct information about the energy release process that boosts the radiating particles to an energy per particle E $\geq$ 25 keV (see Fig. 1).

There is ample evidence that simultaneous impulsive bursts of hard X rays (photon energy range from 25 keV to 500 keV) and microwaves (3 GHz $\leq f \leq$ 100 GHz band) both radiate from one distribution of energetic electrons (Takakura and Kai 1966; Mätzler 1978; Gary 1985; Schmahl, Kundu, and Dennis 1985; Kai 1986). The X rays are bremsstrahlung and the microwaves are gyrosynchrotron radiation. Crannell *et al.* (1978) made the assumption of a common source electron distribution, interpreted the hard X-ray spectra as thermal bremsstrahlung, and introduced a method to derive a characteristic length scale of a burst source. Their analysis showed that the rise times of solar impulsive bursts were correlated with spatial length scales of the sources. The correlation was confirmed by Batchelor *et al.* (1985) and Batchelor (1987), using *SMM* observations of hard X rays and microwave observations from Bern, Toyokawa, and Itapetinga observatories. The correlation is linear, consistent with the thermal conduction front model (TCF, see Brown, Melrose, and Spicer 1979).

A similar method for deriving source lengths was used in the work described herein, but it was adapted for use with *nonthermal* source models. The observations analyzed by Batchelor *et al.* (1985) and Batchelor (1987) were re-analyzed, employing the standard nonthermal models in the literature, the thick-target model (TT, Brown 1971) and trap-plus-precipitation model (TP, Melrose and Brown 1976).

II. METHOD OF ANALYSIS

The analysis method is briefly described in this section; a more detailed description of the method was given by Batchelor *et al.* (1985) and Batchelor (1989). The hard X-ray observations were made with the Hard X-ray Burst Spectrometer (HXRBS, see Orwig, Frost, and Dennis 1980). The microwave observations were made at Bern (Magun *et al.* 1981), Toyokawa (Torii *et al.* 1979), and Itapetinga (Kaufmann *et al.* 1982).

If the microwave spectrum of a burst is known throughout a sufficiently broad band, it generally exhibits a low-frequency segment with positive spectral index α (*i.e.* flux density $S \propto f^{\alpha}$, where f is frequency in Hz) and a high-frequency segment with negative α (the full spectrum is termed "C-type", Guidice and Castelli 1975; see Fig. 2 for examples). The positive-α segment is usually attributable to emission that is optically thick, due to self-absorption, and the negative-α segment to emission that is

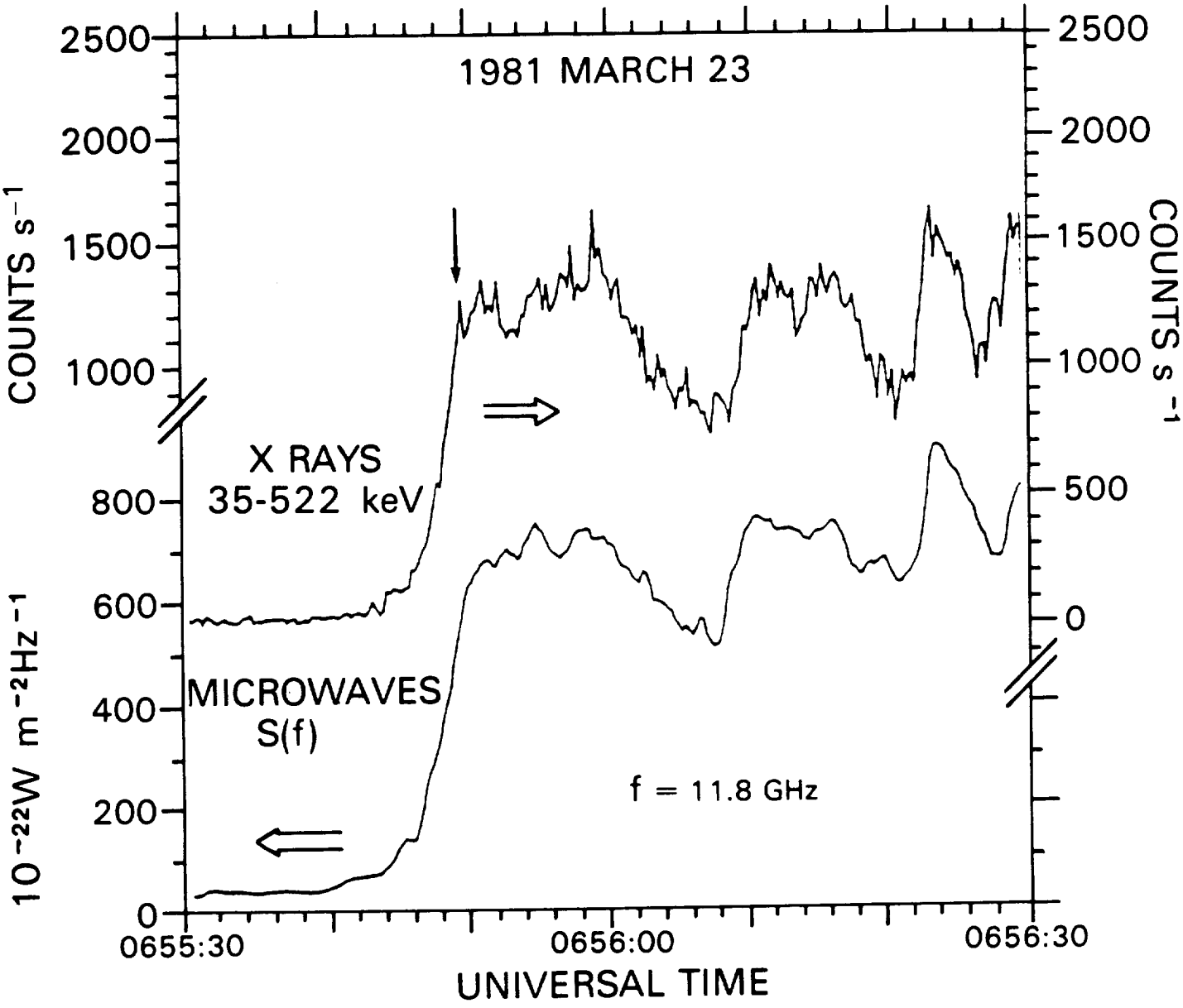

Figure 1. An impulsive solar burst of hard X rays and microwaves (HXRBS and Bern data respectively). The descending arrow marks the end of the first steady, impulsive rise during this burst, and the flux at this time was used to determine t_r (see text).

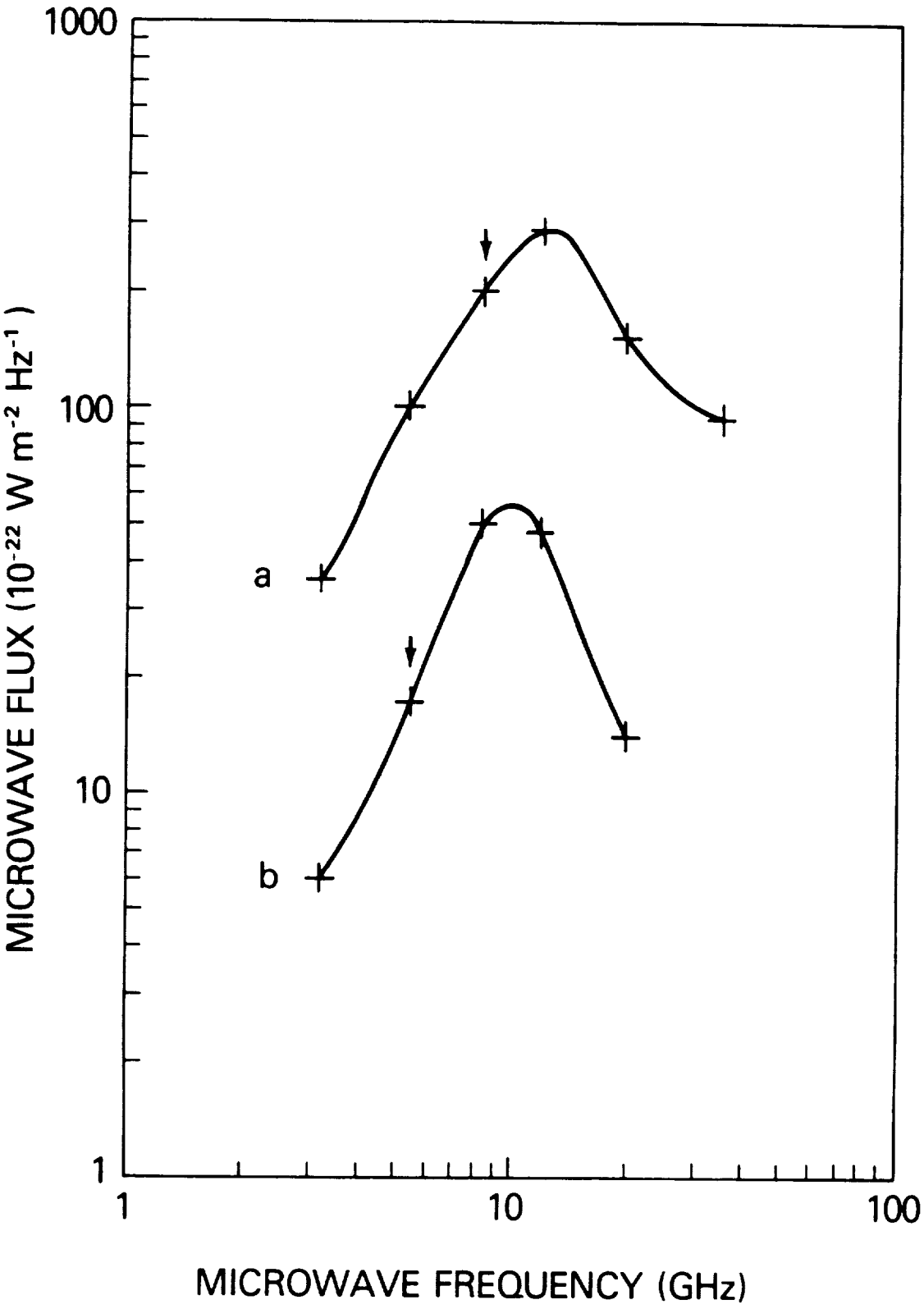

Figure 2. Examples of two microwave burst spectra, each at the time of hard X-ray burst maximum (Bern data). (a) 1981 August 10, (b) 1981 May 4. Arrows indicate points used to determine S_2 and f_2 (see text).

optically thin (Mätzler 1978; Ramaty 1969). The optically-thick emission was used here to derive an area of each source at the time when the counting rate summed over the whole HXRBS energy range was maximum.

First, 30 bursts observed with HXRBS and the radiotelescopes were selected. Bursts were selected with steady rises to a peak or plateau in their time histories ($t_r \leq$ 30 s), and microwave spectra observed in the positive-α segment. (Twice the time from half-maximum to maximum was defined as t_r.) For each burst, values denoted S_2 and f_2 were selected at the highest-frequency observation on the positive-α segment (see Fig. 2). The X-ray spectrum from HXRBS of each burst at its peak flux was fitted with the power law $I(\varepsilon) = A_1\ \varepsilon^{-\gamma}$ photons cm^{-2} s^{-1} keV^{-1}, in order to obtain the hard X-ray spectral index γ.

The approximate formulae derived by Dulk and Marsh (1982) for optically-thick microwave flux from a power law distribution of electrons ($N(E) \propto E^{-\delta}$ electrons cm^{-3}) were used to compute the effective emission temperature of the nonthermal microwave source T_{eff} (deg K) and A, the area of each source (cm^2):

$$T_{eff} = 2.2 \text{ x } 10^9\ 10^{-0.31\ \delta} \cdot$$

$$\cdot\ (\sin\ \theta)^{-0.36-0.06\ \delta}\ (f/f_B)^{0.50+0.085\ \delta} \qquad (1)$$

$$A = 7.5 \text{ x } 10^{43}\ S\ f^{-2}\ T_{eff}^{-1}, \qquad (2)$$

In Eq. (1), δ is the power-law index of the electron distribution. In the TT model, $\delta = \gamma + 1$, and in the TP model, $\delta = \gamma - \frac{1}{2}$. B is the magnetic field, the variable f_B = 2.8 x 10^6 B is the gyrofrequency (Hz), and θ is the angle between the **B** vector and the line of sight. In Eq. (2), the Sun-Earth distance is accounted for, and the units of S are solar flux units (1 SFU = 10^{-22} W m^{-2} Hz^{-1}).

The uncertainties in B and θ were treated as follows. Typical values of B in flares, deduced from other solar observations, generally range from 100 to 1000 gauss (Švestka 1976; Brown, Smith, and Spicer 1981). In this work, two values of $L \equiv A^{1/2}$ were computed for each burst, with B set equal to each of those two limits; the range in results was treated as the $\pm 1\sigma$ uncertainty. L is admittedly a crude approximation of the characteristic source dimensions, but its large range of variation – more than three orders of magnitude – makes it useful despite uncertainties in length-to-width ratio of the sources that it incorporates. The angle θ could not be measured. Gyrosynchrotron radiation is emitted most intensely in directions $\approx 90°$ from **B** (see Eq. (1)), so that the part of each source with θ nearest to 90° contributes most of the radiation. The dependence of L on θ is slight in the range $45° \leq \theta \leq 90°$, so $\theta = 45°$ was assumed for each burst, as an estimate of the mean value. Little error is incurred since bursts with small θ would have low T_{eff}, and tend not to be observed.

III. RESULTS

The observational parameters and results appear in Table 1. Figure 3 shows the plot of L vs. t_r for the TT model. The TP results make a very similar plot in Figure 4, except for a reduction of the L values by about 30%. Three of the flares occurred on or beyond the solar limb, and are marked with square symbols. Because these bursts might have been partially occulted by the limb, altering A, only the other 27 were included in the least-squares fit (Bevington 1969), drawn as the straight line in the plot. The slope of the best fit line, 1.07 ± 0.05, is unity within the uncertainties.

At least one of the limb bursts, the 1981 Dec. 7 event, has a value of L that is markedly displaced from the correlation, appearing in Fig. 3 with a square symbol well below the best fit line. The displacement of its value of L is in the direction consistent with partial occultation of a flare located just beyond the solar limb. This is an important test of consistency in the interpretation of A as representative of the true source area; displacement of a limb flare value of L in the other direction relative to unocculted burst values would have been an unresolvable conflict with geometry.

As described by Batchelor *et al.* (1985), the parameters entering the correlation were checked to reveal possible more fundamental underlying correlations. Of particular concern was the "Big Flare Syndrome" (Kahler 1982), the possible association of larger flare intensities with larger source sizes, harder X-ray spectra, etc. No underlying parameter correlations were capable of accounting for the close least-squares fit of the relation in Fig. 3. The "Big Flare Syndrome" in particular was ruled out by broad scatter in the plot of S_2 vs. t_r.

IV. DISCUSSION

The deduction that $L \propto t_r$ if one chooses the TT or TP model has important implications for the interpretation of impulsive flare phenomena. The correlation of L with t_r was already known on the basis of thermal flare models. The differences between thermal and nonthermal models for impulsive microwave and X-ray emission are substantial, and the (L, t_r) correlation must result in disparate ways from each of these models. The key inference from these results is: whether one chooses a model from either the nonthermal or thermal alternatives, there is clear evidence in each case that all impulsive bursts in the $0.1 \leq t_r \leq 30$ s range are due to one *type* of causative agent, characterized by a velocity of order 10^8 cm s^{-1}. A precise single velocity for the agent is not implied by the data, of course, given the crudeness of L and the scatter of the values; nevertheless, a *type* of agent that travels at speeds within less than an order of magnitude range is suggested by Fig. 3, and this will be termed "a characteristic velocity" hereafter.

TABLE I

Observational and Derived Parameters
of Solar Hard X-ray/Microwave Bursts

Date	UT	γ	t_r (s)	S_2 (SFU)	f_2 (GHz)	L TT model (cm)	L TP model (cm)
80 Mar 29	0918:09	3.3	3.0	510.	10.4	6.5×10^8	4.4×10^8
80 Mar 29	0955:06	2.8	5.2	210.	10.4	3.6×10^8	2.5×10^8
80 Jun 04	0654:19	3.8	7.0	320.	8.4	8.0×10^8	5.3×10^8
80 Jun 29	1041:35*	3.6	3.6	31.	8.4	2.4×10^8	1.6×10^8
80 Jul 01	1626:53	2.8	0.8	135.	19.6	1.2×10^8	8.4×10^7
80 Jul 01	1626:56	2.9	0.9	460.	19.6	2.3×10^8	1.6×10^8
80 Jul 01	1626:59	3.2	0.8	39.	19.6	7.1×10^7	5.0×10^7
80 Jul 01	1627:02	2.8	1.0	82.	35.0	4.1×10^8	3.0×10^7
80 Jul 01	1627:04	3.0	0.8	486.	28.0	1.4×10^8	1.0×10^8
80 Jul 01	1627:08	2.6	1.0	894.	35.0	1.3×10^8	9.5×10^7
80 Jul 01	1627:13	2.6	1.4	1330.	35.0	1.6×10^8	1.2×10^8
80 Oct 09	1123:58	4.2	5.2	100.	5.2	1.0×10^9	6.5×10^8
80 Nov 05	2233:02	3.8	24.	2400.	9.4	1.9×10^9	1.2×10^9
80 Nov 06	0650:51	4.5	20.	910.	8.4	1.6×10^8	1.1×10^9
80 Nov 08	1450:25	5.9	7.	33.	8.4	4.6×10^7	3.0×10^8
80 Nov 18	0718:08*	3.4	2.2	44.	19.6	7.9×10^8	5.5×10^7
80 Dec 17	0845:37	3.2	3.2	280.	8.4	6.3×10^8	4.2×10^8
81 Mar 23	0655:49	3.5	6.0	260.	8.4	6.6×10^8	4.4×10^8
81 Apr 10	1644:53	4.3	10.	120.	5.2	1.1×10^9	7.3×10^8
81 Apr 15	0643:09	4.7	3.8	14.	5.2	4.4×10^8	2.8×10^8
81 Apr 18	1049:28	4.5	5.0	55.	8.4	4.0×10^8	2.7×10^8
81 Apr 26	1115:31	4.	11.	75.	3.2	1.7×10^9	1.0×10^9
81 May 04	0838:03	4.2	1.8	17.	5.2	4.2×10^8	2.7×10^8
81 Jul 19	0533:25	3.9	12.	1400.	19.6	5.0×10^9	3.5×10^8
81 Jul 20	1311:27	4.5	22.	170.	2.8	3.6×10^9	2.2×10^9
81 Aug 10	0658:50	3.9	2.6	200.	8.4	6.5×10^8	4.3×10^8
81 Dec 07	1451:02*	3.1	10.0	240.	19.6	1.7×10^8	1.2×10^8
84 May 21	1326:29	2.7	0.2(m)	20.	90.0	5.3×10^6	4.1×10^6
84 May 21	1326:30	2.4	0.1(m)	50.	90.0	7.9×10^6	6.1×10^6
84 May 21	1326:37	3.2	0.1(m)	30.	90.0	7.0×10^6	5.4×10^6

* Limb flares, excluded from length-rise time correlation due to possible limb occultation.

m The 1984 May 21 bursts had rise times shorter than HXRBS time resolution. The microwave rise time has therefore been used. In all other cases, the rise time is derived from HXRBS data.

LENGTHS VS. RISE TIMES: THICK TARGET

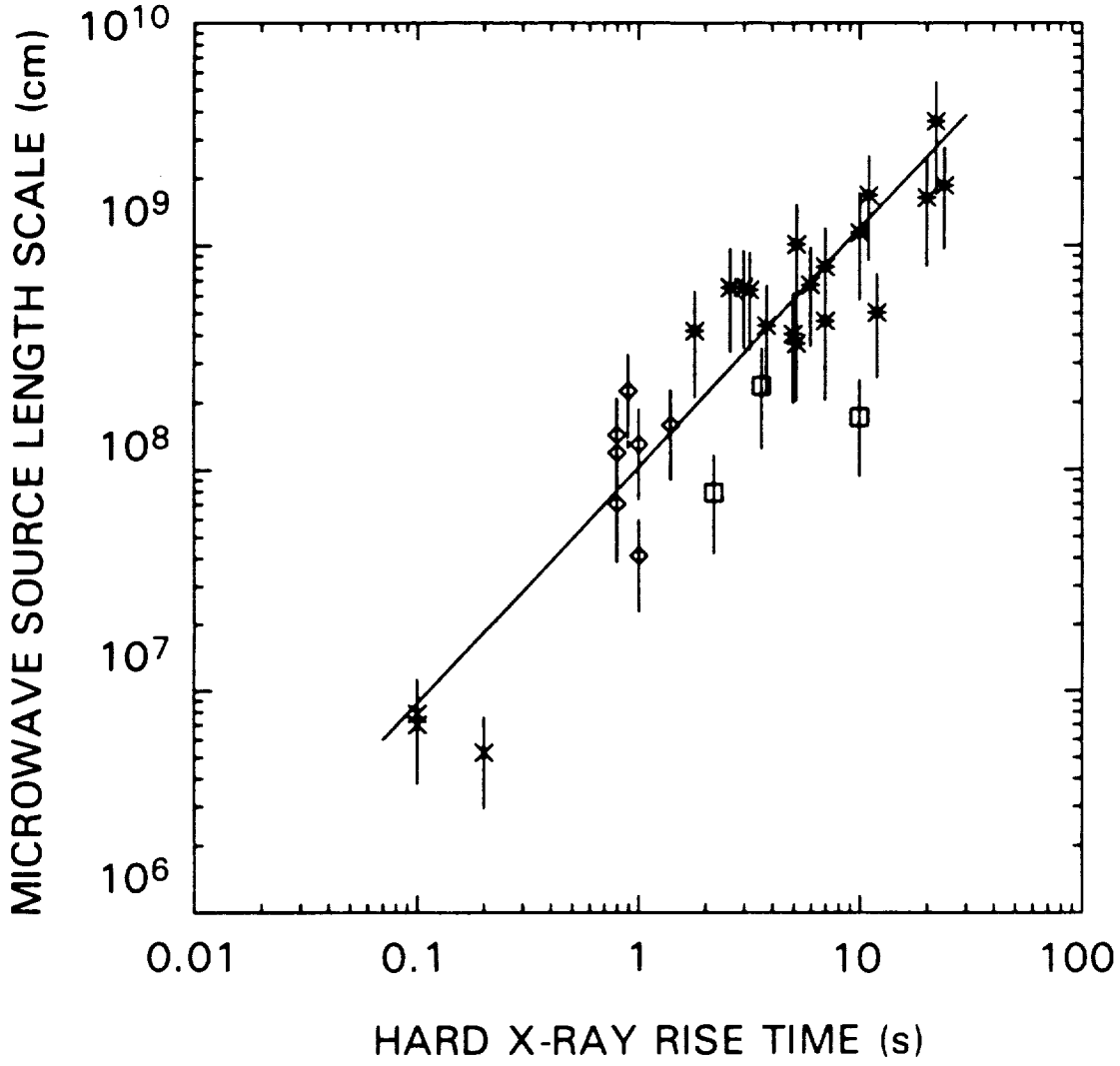

Figure 3. Plot of burst source length scales L vs. rise times t_r, assuming the TT model. Symbols: crosses label three bursts from the 1984 May 21 flare observed at Itapetinga; diamonds label seven bursts from the 1980 July 1 flare; all other symbols label bursts from other flares. Squares indicate limb events; because these bursts might have been partially occulted (reducing L), they were excluded from the least-squares fit. The fit, performed with the function $log\ L = log\ a\ +\ b\ log\ t_r$, yielded $a = 10^8$ cm s^{-1}, $b = 1.07$, $\sigma_{log\ a} = 0.08$, $\sigma_b = 0.05$, correlation coefficient $r = 0.95$. There are N = 27 points, so the probability that the quantities L and t_r are actually uncorrelated is $P_c(r, N) \ll 10^{-6}$.

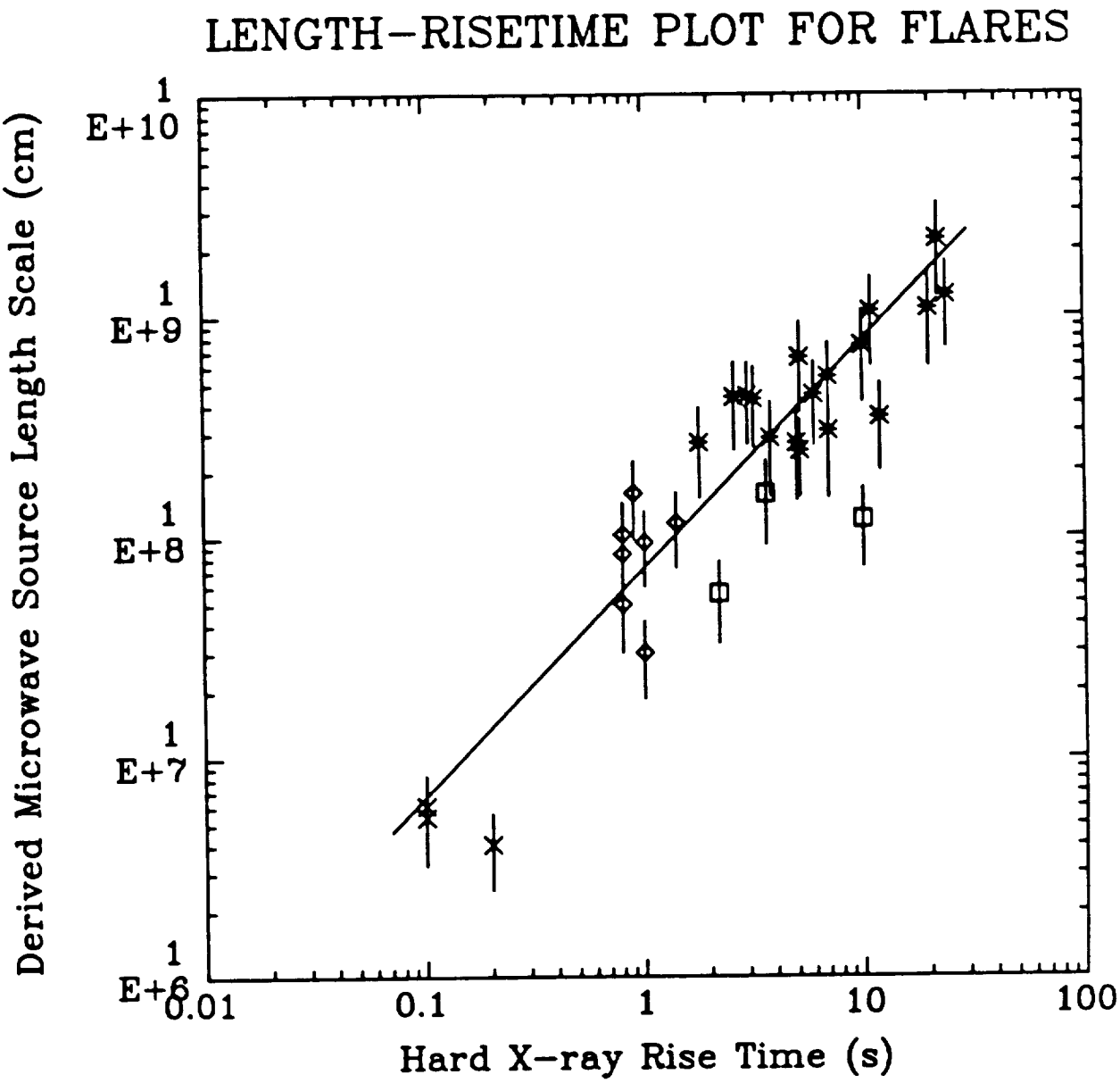

Figure 4. Same as Fig. 3 for the trap-plus-precipitation (TP) model. The fit parameters are similar: $a = 7.3 \times 10^7$ cm s^{-1}, $b = 1.03$, $\sigma_{log\ a} = 0.07$, $\sigma_b = 0.04$, correlation coefficient $r = 0.95$. Again with N = 27 points, the probability that the quantities L and t_r are actually uncorrelated is $P_c(r, N) \ll 10^{-6}$.

The nature of the causative agent and its characteristic velocity are specific to each model. The mean values are 10^8 cm s^{-1} for the TT model, 7 x 10^7 cm s^{-1} for the TP model, and 2 x 10^8 cm s^{-1} for the TCF model. In each model, the role of this agent is fundamental: it couples the energy release process to the geometrical scale of the burst source region and determines the duration of the most rapid impulsive energy release phase. Possible agents are shocks in the nonthermal models and TCFs. Any other processes of flare energy release that may be proposed also must include such an agent.

Perhaps it is no great surprise that a velocity of order 10^8 cm s^{-1} characterizes the growth of flare sources, but this has not been demonstrated heretofore by means of standard *nonthermal* models, nor has the dependence of the characteristic velocity on the chosen model been derived before. One can envision many ways that flare sources could grow with some characteristic speed, so the results described above do not permit us to discriminate between models. Nevertheless, the evidence for interpretation of the burst rise time as a phase of growing source area is an important departure from the long-standing interpretation that the time behavior of the injection of accelerated particles, convolved with particle propagation effects, determines burst rise times (*e.g.*, Emslie 1983; Lu and Petrosian 1988).

The results of this work suggest other new lines of investigation. First, the correlation $L \propto t_r$ supports the future use of A and L measurements as meaningful tools of source analysis, whereas they were more questionable before. Future studies may benefit from tests for correlations between L or A and other available flare parameters. Second, the causal agent responsible for the correlation must be thought of as a physical process that can operate in a similar manner on size scales that vary by three orders of magnitude, a useful datum for investigations of simulated flare energy release via magnetic reconnection. Conversely, something must serve to terminate the process on equally wide-ranging size scales. Third, these results give information about a few sources that are less than one arc second in angular size. Even the most advanced microwave imaging system for flares, the Very Large Array, can't provide such information with its images.

The clear evidence herein for source growth with a characteristic velocity during burst rises should be tested with spatially-resolved observations. Most of the bursts in this study had rise times too short for observations of their progressive growth with the VLA, given its 10-s time resolution. Comparisons of the source areas from the VLA with burst rise times are possible and would provide an important test of these results.

CONCLUSION

- Max '91 study of impulsive hard X-ray/microwave bursts should focus on identifying the causative agent suggested herein
- Combined images in hard X rays and microwaves (*e.g.* GRID/VLA) should be used to search for the following phenomena:
  * Shock acceleration
  * Thermal conduction fronts
  * Traveling magnetic reconnection instabilities
- These possible causative agents should reveal themselves via their distinctive relationships with coronal magnetic structures
  * Quasi-perpendicular orientation of field lines relative to a radially expanding disturbance
  * Conductive growth of hot sources longitudinally along field lines
  * Longitudinal source expansion at speed near Alfvén velocity

ACKNOWLEDGEMENTS

The author is very grateful to the HXRBS team and to the solar observers at Bern Radio Observatory, Toyokawa Observatory and Itapetinga Observatory for permission to use their data and for advice in the analysis. Critical reading of the manuscript by C.J. Crannell and B.R. Dennis is also appreciated.

REFERENCES

Batchelor, D.A., Crannell, C.J., Wiehl, H.J., and Magun, A. 1985, *Ap. J.*, **295**, 258.

Batchelor, D.A. 1987, in *Rapid Fluctuations in Solar Flares, NASA Conference Publication 2449*, eds. Dennis, B.R., Orwig, L.E., and Kiplinger, A.L., (NASA, Washington, 1987), p. 35.

Batchelor, D.A. 1989, *Ap. J.*, **340**, 607.

Bevington, P.R. 1969, *Data Reduction and Error Analysis for the Physical Sciences*, (McGraw-Hill, New York), Chap. 6.

Brown, J.C. 1971, *Solar Phys.*, **18**, 489.

Brown, J.C., Melrose, D.B., and Spicer, D.S. 1979, *Ap. J.*, **228**, 592.

Brown, J.C., Smith, D.F., and Spicer, D.S., 1981, in *The Sun as a Star, NASA Special Pub. 450*, ed. Jordan, S. (NASA, Washington), p. 181.

Crannell, C.J., Frost, K.J., Mätzler, C., Ohki, K., and Saba, J.L. 1978, *Ap. J.*, **223**, 620.

Dulk, G.A., and Marsh, K.A. 1982, *Ap. J.*, **259**, 350.

Emslie, A.G. 1983, *Ap. J.*, **271**, 367.

Gary, D.E. 1985, *Ap. J.*, **297**, 799.

Guidice, D.A., and Castelli, J.P. 1975, *Solar Phys.*, **44**, 155.

Kahler, S.W. 1982, *J. Geophys. Res.*, **87** (A5), 3439.

Kai, K. 1986, *Solar Phys.*, **104**, 235.

Kaufmann, P., Strauss, F.M., Schaal, R.E., and Laporte, C. 1982, *Solar Phys.*, **78**, 389.

Lu, E.T., and Petrosian, V. 1988, *Ap. J.*, **327**, 405.

Magun, A., Fuhrer, M., Kaempfer, N., Staeli, M., Schöchlin, W., and Wiehl, H. 1981, *Institute for Applied Physics Rept. 46* (University of Bern, Switzerland).

Mätzler, C. 1978, *Astron. Astrophys.*, **70**, 181.

Melrose, D.B., and Brown, J.C. 1976, *Mon. Not. R. Astron. Soc.*, **176**, 15.

Orwig, L.E., Frost, K.J., and Dennis, B.R. 1980, *Solar Phys.*, **65**, 25.

Ramaty, R. 1969, *Ap. J.*, **158**, 753.

Schmahl, E.J., Kundu, M.R., and Dennis, B.R. 1985, *Ap. J.*, **299**, 1017.

Švestka, Z. 1976, *Solar Flares* (Reidel, Dordrecht), pp. 176-180.

Takakura, T., and Kai, K. 1966, *Publ. Astron. Soc. Japan* **18**, 57.

Torii, C. 1979, *et al. Proc. Res. Inst. Atmos. Nagoya Univ.*, **26**, 129.